Retrieval of Tropical Cirrus Cloud Properties from Ground-Based Lidar and Millimeter-Wave Radar Sensing at the Maritime Continent Thunderstorm Experiment

R. T. Austin, S. A. Young, C.M.R. Platt and G. R. Patterson
CSIRO, Division of Atmospheric Research
Aspendale, Victoria, Australia

S. M. Sekelsky and R. E. McIntosh
Microwave Remote Sensing Laboratory
University of Massachusetts
Amherst, Massachusetts

Introduction

The Maritime Continent Thunderstorm Experiment (MCTEX) was conducted in November and December 1995 on Melville and Bathurst Islands, north of Darwin off the northern coast of Australia. Scientists from CSIRO and the University of Massachusetts (UMass) made simultaneous, collocated measurements of lidar backscatter and radar reflectivity of synoptic cirrus and cirrus outflows from island thunderstorms using instruments based at Pularumpi (Garden Point), Melville Island (11° 24′ S, 130° 25′ E—see Figure 1). This abstract presents comparisons of cloud structure as detected by the two instruments, showing their relative abilities to measure high, thin cirrus layers and strongly attenuating anvil clouds. We also describe current progress in the retrieval of cirrus particle size parameters through the combination of lidar and radar backscatter data.

Introduction

Organized by the Australian Bureau of Meteorology, MCTEX was designed to provide multiple opportunities to measure clouds associated with "Hectors"—intense thunderstorms occurring almost daily over Melville and Bathurst Islands during the "build-up" period prior to the onset of the monsoon season in December. The CSIRO and UMass teams deployed their instruments together at Pularumpi to observe the cirrus outflows from these storms.

The CSIRO multi-wavelength scanning polarization lidar measured backscatter profiles at intervals of 30 to 60 seconds. Recorded profiles were usually averages of 16 to 256 lidar shots (1.6 to 26 seconds). Simultaneous measurements of

Figure 1. The Tiwi Islands (Melville and Bathurst) lie off Australia's northern coast. The instruments were situated at Pularumpi, on the west coast of Melville Island.

infrared radiance were collected by the Division of Atmospheric Research (DAR) Atmospheric Radiation Measurement (ARM) radiometer at 10.86 μm. The lidar and radiometer recorded vertically, observing the same cloud volume for lidar and infrared radiometer (LIRAD) retrievals of cloud backscatter coefficient (see Platt [1979] and the related abstract by Platt et al. in this volume).

The UMass Cloud Profiling Radar System (CPRS) operates at 33 GHz (Ka-band) and 95 GHz (W-band). Both channels transmit and receive through a single 1-meter diameter dielectric lens antenna and can measure polarimetric quantities such as Z_{DR} and differential phase constant. A comparison of the lidar and radar specifications is given in Table 1.

Table 1. CSIRO lidar and UMass CPRS instrument characteristics.

	Lidar	W-band radar	Ka-band radar
Wavelength	532 nm	3.16 mm	9.05 mm
Peak power	25 MW	1.5 kW	120 kW
Maximum avg. power	1.5 W	15 W	120 W
PRF	10 Hz	1 Hz-20 kHz	200-3000 Hz
Pulse width	6 ns	50-2000 ns	200-2000 ns
3 dB beamwidth	0.03°	0.2°	0.5°
Rec. aperture field of view	2, 5, 10 mrad		

Relative Sensitivity

The variety of cirrus clouds observed at MCTEX provided an ample demonstration of the relative strengths and weaknesses of the lidar and millimeter-wave radar in sensing cirrus cloud properties. The instruments are complementary in their abilities.

Lidar observations on seemingly clear days during MCTEX revealed very thin layers of cirrus near the tropopause. These layers were detected in almost every lidar data set when not masked by lower clouds. Neither the Ka-band nor the W-band radar was able to detect these layers.

Slightly more dense cirrus clouds became partially visible to the Ka-band radar. This radar experiences less attenuation than the W-band radar (mostly due to water vapor) and is therefore preferred in these comparisons. A comparison of the lidar cloud backscatter coefficient and radar reflectivity for a low-density (optically thin) cirrus case is shown in Figure 2.

Several cases of medium-density cirrus had measurable radar reflectivities, yet were not thick enough to prevent complete penetration by the lidar pulses. Cloud features and boundaries appear roughly similar in these cases, considering the different temporal and vertical resolution of the two sensors. Examples of lidar and Ka-band radar views of such clouds are shown in Figure 3.

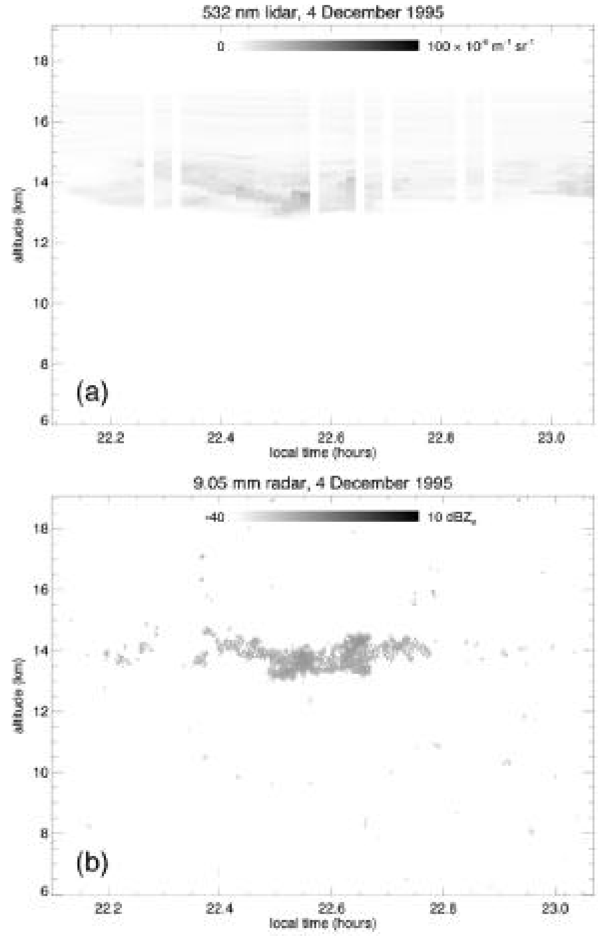

Figure 2. Time-height diagrams of (a) lidar differential backscatter coefficient and (b) Ka-band radar reflectivity for some low-density cirrus layers.

The lidar was unable to penetrate very dense (optically thick) anvil outflows observed on a couple of occasions. The millimeter-wave radar was not so limited, returning useable signals through to the top of the anvil, much deeper than the 1–2 km seen by the lidar. Lidar and Ka-band radar profiles of a dense anvil cloud are shown in Figure 4.

Retrieval of Size Information

Numerous techniques have been proposed using dual-sensor data sets (e.g., dual-wavelength radar, radar, and radiometer) to infer characteristics of the particle size distribution as a

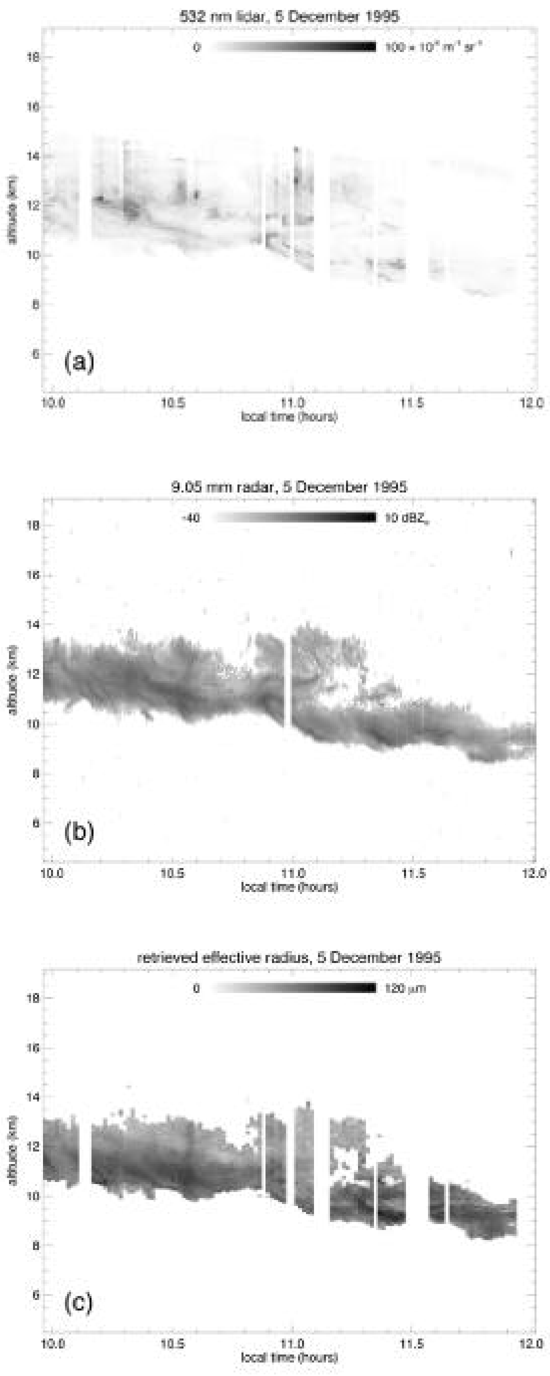

Figure 3. Time-height diagrams of (a) lidar differential backscatter coefficient, (b) Ka-band radar reflectivity for some low-density cirrus layers, and (c) retrieved effective radius for medium-density cirrus.

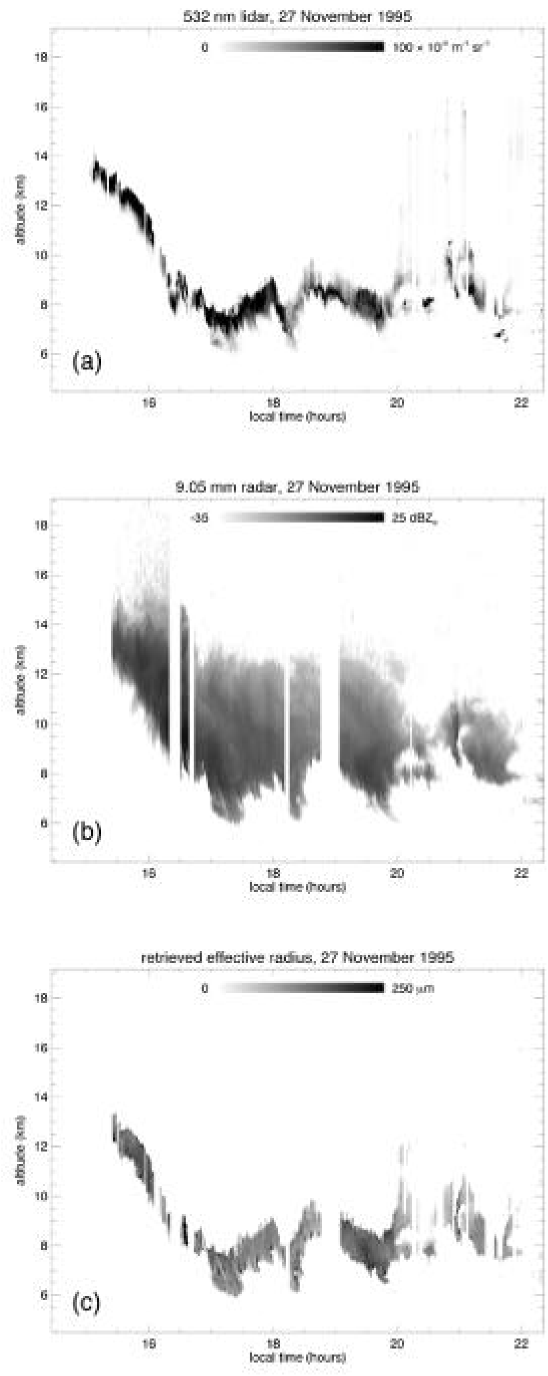

Figure 4. Time-height diagrams of (a) lidar differential coefficient, (b) Ka-band radar reflectivity, and (c) retrieved effective radius for dense (optically thick) anvil cirrus.

function of position within a cirrus cloud (Matrosov 1993; Matrosov et al. 1994; Intrieri et al. 1993). These techniques assume some form of distribution function and particle shape (and corresponding phase function) and use the dual data sets to retrieve particular parameters or moments of the distribution.

Data from the lidar and millimeter-wave radar at MCTEX were used to perform such a retrieval. In an analysis similar to that of Intrieri et al. (1993), we assume a modified gamma distribution of spherical ice particles (Figure 5):

$$n(r) = \frac{N_0}{\Gamma(p) r_m} \left(\frac{r}{r_m} \right)^{p-1} \exp\left(\frac{-r}{r_m} \right),$$

where $n(r)$ = the number of particles of radius r to r + dr per cubic meter
N_0 = the number density,
Γ = the gamma function,
p = the dispersion factor
r_m = the characteristic radius of the distribution.

The effective radius r_e, defined as the ratio of the volume of all particles in the size distribution to their geometrical cross-sectional area, is related to the characteristic radius r_m by $r_c = (p+2) r_m$.

Using the assumption of ice spheres, the backscatter coefficients β_{lidar} and β_{radar} at lidar and Ka-band radar wavelengths can be calculated using a Mie scattering code for a modified gamma distribution of particles as a function of effective radius. The logarithm of the ratio of these coefficients is related to the effective radius of the distribution as shown in Figure 6. (The equation of fit is based on a modified gamma modified gamma distribution with p = 5, but changing p to 2 has little effect.) Note that this relation is independent of the number density N_0.

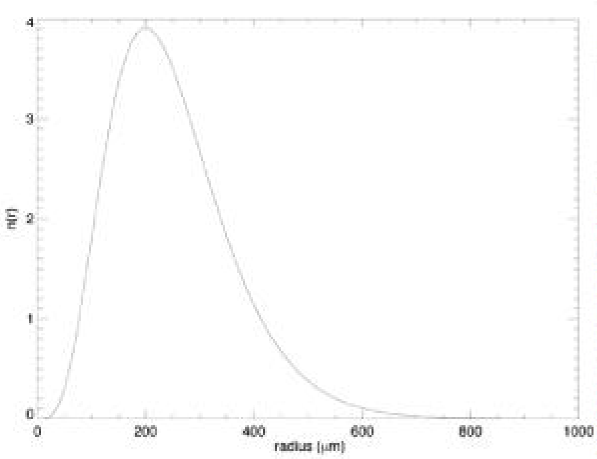

Figure 5. A modified gamma distribution was assumed for the particle size distribution in this analysis.

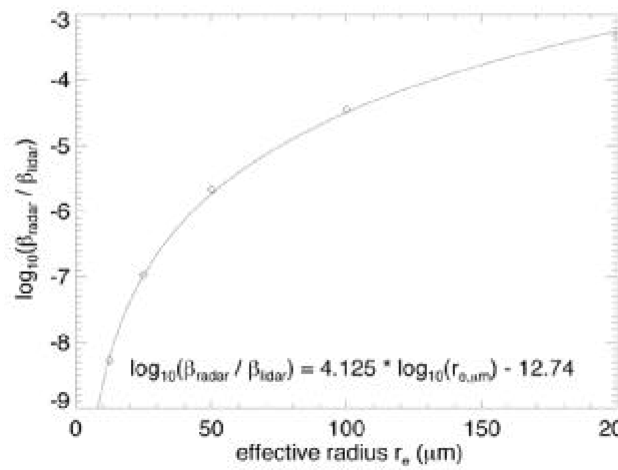

Figure 6. Derived relation between the radar/lidar ratio and the effective radius.

Using the equation of fit, measured values of the lidar and radar backscatter coefficients were used to estimate the effective radius of MCTEX cirrus clouds as a function of position within the cloud. Radar data were interpolated to lidar spatial and temporal resolutions, and reflectivity values were converted to backscatter coefficients. Examples of estimated effective radius are shown in Figures 3c and 4c.

Discussion

The combination of lidar and millimeter-wave radar backscatter shows potential in the retrieval of cirrus particle size information. While there were no in situ measurements of cloud crystal sizes at MCTEX, we hope to compare lidar/radar size retrievals with aircraft measurements at a future intensive observation period (IOP).

The examples shown here rely on simple assumptions, which need to be replaced with more accurate descriptions. For example, cirrus crystals are not spherical, but appear as plates, columns, and more complex habits. Work on similar retrievals using cylinders and plates is in progress. Work is also proceeding on the use of different particle size distribution functions, such as the Marshall-Palmer or Heymsfield-Platt power-law distribution functions (Houze et al. 1979; Heymsfield and Platt 1984; Platt 1997).

An obvious limitation of the technique is that sufficient lidar and radar signal levels are required. This becomes both an upper and lower limit to cloud density—optically thin clouds will be invisible to the radar, while optically thick clouds will block lidar sensing of all but the lowest layers (e.g., Figure 4c). An alternative technique in the case of optically thick clouds is the use of millimeter-wave and microwave radars, as described by Sekelsky et al. (this volume).

Acknowledgments

The authors thank the Bureau of Meteorology MCTEX Science Team for their logistical and moral support of the ARM experiment. The research was supported under the U.S. Department of Energy, Office of Health and Environmental Research, Grant No. DE-FG02-92ER61373.

References

Heymsfield, A. J., and C.M.R. Platt, 1984: A parameterization of the particle size spectrum of ice clouds in terms of the ambient temperature and the ice water content. *J. Atmos. Sci.,* **41**, 846–855.

Houze, Jr., R. A., P. V. Hobbs, P. H. Herzegh, and D. B. Parsons, 1979: Size distributions of precipitation particles in frontal clouds. *J. Atmos. Sci.*, **36**, 156–162.

Intrieri, J. M., G. L. Stephens, W. L. Eberhard, and T. Uttal, 1993: A method for determining cirrus cloud particle sizes using lidar and radar backscatter technique. *J. Appl. Meteor.*, **32**, 1074–1082.

Matrosov, S. Y., 1993: Possibilities of cirrus particle sizing from dual-frequency radar measurements. *J. Geophys. Res.*, **98**, 20 675–20 683.

Matrosov, S. Y., B. W. Orr, R. A. Kropfli, and J. B. Snider, 1994: Retrieval of vertical profiles of cirrus cloud microphysical parameters from doppler radar and infrared radiometer measurements. *J. Appl. Meteor.*, **33**, 617–626.

Platt, C.M.R., 1997: A parameterization of the visible extinction coefficient of ice clouds in terms of the ice/water content. *J. Atmos. Sci.*, in press.

Platt, C.M.R., 1979: Remote sounding of high clouds: I. Calculation of visible and infrared optical properties from lidar and radiometer measurements. *J. Appl. Meteor.*, **18**, 1130–1143.

Platt, C.M.R., S. A. Young, R. T. Austin, G. R. Patterson, and S. C. Marsden, 1997: The optical properties of tropical cirrus clouds in MCTEX from lidar and infrared radiometer (LIRAD) retrievals. *Proceedings of the Seventh Atmospheric Radiation Measurement (ARM) Science Team Meeting, March 3–7, 1997, San Antonio, Texas*, CONF-970365, U.S. Department of Energy, Washington, D.C.

Sekelsky, S. M., R. E. McIntosh, W. L. Ecklund, and K. S. Gage, 1997: Neural network estimation of particle size distribution parameters in ice-phase clouds using three frequency radar measurements. *Proceedings of the Seventh Atmospheric Radiation Measurement (ARM) Science Team Meeting, March 3–7, 1997, San Antonio, Texas*, CONF-970365, U.S. Department of Energy, Washington, D.C.